Journal of Zhejiang University-SCIENCE A (Applied Physics & Engineering)
ISSN 1673-565X (Print); ISSN 1862-1775 (Online)
www.zju.edu.cn/jzus; www.springerlink.com
E-mail: jzus@zju.edu.cn

A new principle and device for large aircraft components gaining accurate support by ball joint*

Bao-gui QIU†, Jun-xia JIANG†‡, Ying-lin KE

(*The State Key Laboratory of Fluid Power Transmission and Control, Zhejiang University, Hangzhou 310027, China*)

†E-mail: qiubaogui@zju.edu.cn; junxia.jiang@126.com

Received Mar. 23, 2010; Revision accepted Aug. 18, 2010; Crosschecked Apr. 20, 2011

Abstract: How to obtain an accurate support for large components by ball joint is a key process in aircraft digital assembly. A novel principle and device is developed to solve the problem. Firstly, the working principle of the device is introduced. When three or four displacement sensors installed in the localizer are touched by the ball-head, the spatial relation is calculated between the large aircraft component's ball-head and the localizer's ball-socket. The localizer is driven to achieve a new position by compensation. Relatively, a support revising algorithm is proposed. The localizer's ball-socket approaches the ball-head based on the displacement sensors. According to the points selected from its spherical surface, the coordinates of ball-head spherical center are computed by geometry. Finally, as a typical application, the device is used to conduct a test-fuselage's ball-head into a localizer's ball-socket. Positional deviations of the spherical centers between the ball-head and the ball-socket in the *x*, *y*, and *z* directions are all controlled within ±0.05 mm under various working conditions. The results of the experiments show that the device has the characteristics of high precision, excellent stability, strong operability, and great potential to be applied widely in the modern aircraft industry.

Key words: Aircraft digital assembly, Large aircraft component, Accurate support, Ball joint, Displacement sensor, Three coordinate numerical control localizer

doi:10.1631/jzus.A1000110 **Document code:** A **CLC number:** V26

1 Introduction

Parts shape and size are transferred in the form of an analogue value according to a physical model (Fan, 2001), and a large number of fixtures are applied to locate and clamp components in traditional aircraft assembly (Zhang *et al.*, 2009). To meet the requirement of aircraft component's shape design, it is necessary to consider its concrete structure in fixture design, which leads to a complex tool structure. Furthermore, a set of fixtures can only be used for one aircraft object, which results in a great number of fixtures as well as a lack of flexibility (Naing *et al.*, 2001). The high cost and long lead time of traditional aircraft assembly mode make it difficult for aircraft manufacturers to efficiently meet ever-changing market demands, and it has become the weakest link in the aircraft industry (Hartmann *et al.*, 2004).

The developed countries are dedicated to develop aircraft digital assembly technology to reduce the use of special fixtures and increase automation (Liu and Zou, 2008). Aircraft digital assembly is the extension of digital technology from product design and manufacturing to components assembly and final assembly. The product 3D digital model and a unified coordinate system are applied as the digital standard of aircraft assembly, and parts shape and size are transferred in the form of digital value in aircraft digital assembly. Currently various advanced technologies

‡ Corresponding author

* Project supported by the National Natural Science Foundation of China (No. 50905161), the Natural Science Foundation of Zhejiang Province (No. Y1110339), and the Fundamental Research Funds for the Central Universities of China (No. 2010QNA4024)

have been applied in aircraft digital assembly, such as coordination based on digital standard process equipments, digital simulation, laser measurement, digital location, and cooperative control. Conventional jigs have been replaced by automated positioning and alignment systems composed of localizers and laser measurement systems in the digital environment (Williams *et al*., 2000; Xiong *et al*., 2009). Brötje-Automation has developed the automated alignment facilities, including mechanized jacks, integrated laser tracks, control system, and software, to accurately manipulate and position aircraft fuselages (Naing and Corbett, 2004).

A three coordinate numerical control localizer is a jig which can move and locate accurately in the *x*, *y*, and *z* directions. A so-called ball-head is fixed to the large aircraft components, such as fuselages or wings. A so-called ball-socket is installed on the top of the localizer. The ball-head and the ball-socket form the ball joint in aircraft digital assembly. The ball-head can rotate freely relative to the ball-socket in all directions to meet the need of the large aircraft component's spatial position and pose alignment. In general, the large component's weight ranges from several tons to tens of tons, and it should be supported by several localizers in the assembly process. Thus the problem of how to conduct an aircraft component's ball-head into a localizer's ball-socket is involved. If the spherical center of the ball-head coincidences quite well with that of the ball-socket, the ball-socket will apply an upward force to the ball-head, and the aircraft component is safe. If there is obvious positional deviation of the spherical center in the *x* or *y* direction (i.e., the ball-head and the ball-socket do not contact exactly), the ball-socket will apply an unwanted lateral force to the ball-head. As a result, it will cause the large aircraft component's lateral deformation, and affect its position and pose alignment accuracy while its elastic deformations are released. Therefore it is important to study and improve the support method and precision of the large aircraft component.

The laser trackers are used in a number of applications for their high precision and independence of operator skills, such as tooling calibration and surface contour measurement (Kong *et al*., 2005). To gain accurate support for the large aircraft components, an optional method is as follows: operators move the reflector of laser trackers' datum marks to measure 3D coordinates of the ball-head spherical center, and then the localizer will be driven to follow the position above. Obviously, the method is valid only when the state of the large aircraft component is stable, and the problems of low work efficiency, difficult tracing, and heavy workload are generated (Sun *et al*., 2009). In addition, some aircrafts' huge shapes will increase the difficulty of the laser trackers layout design, and there is a certain loss of precision when the coordinate system is brought in from various stations (Saadat and Cretin, 2002).

In this paper, a new device for gaining accurate support for large aircraft components is designed and developed, and a revising algorithm to discover the contacting center is proposed. The device is successfully applied to support a test-fuselage. Positional deviations of the spherical center between the ball-head and the ball-socket in three directions are all controlled within ±0.05 mm under different working conditions. The device can ensure high precision and good security of large component's position and pose alignment. The device has been used successfully not only in components assembly but also in final assembly, such as fuselage sections join, wing boxes join, and wing-to-fuselage join.

2 Device structure and working principle

Fig. 1 shows the basic structure of the device. The device mainly consists of a support plate, an integrated sensor fixation apparatus, four displacement sensors, a ball-socket, a laser emitter support, four or more laser emitters, three fine lock cylinders etc. The support plate is installed on the top of the localizer. The upper surface of the sensor fixation apparatus is fixed to the bottom of the support plate. The four displacement sensors are installed in the sensor fixation apparatus, and distributed uniformly in the circumferential direction of the ball-socket. The positions of the displacement sensors can also be regulated in the *z* direction. The ball-socket is mounted on the step of the support plate. Furthermore, there is an interference fit between the outer wall of the ball-socket and the inner hole of the support plate. The pressure plate is fixed to the upper surface of the support plate. The laser emitter support is installed on the upper surface of the pressure plate. Several laser emitters are distributed uniformly in the circumferential direction of the laser emitter support. The ball-head and the transition joint are connected by bolts. The transition joint is fixed to the large aircraft component. The ball-head and the ball-socket form the ball joint, enabling the large aircraft component to rotate freely relative to the localizers. Three fine lock cylinders are installed on the lateral support plate. Piston rods, driven by a flow of compressed air, propel locking pins to clamp or unclamp the ball-head.

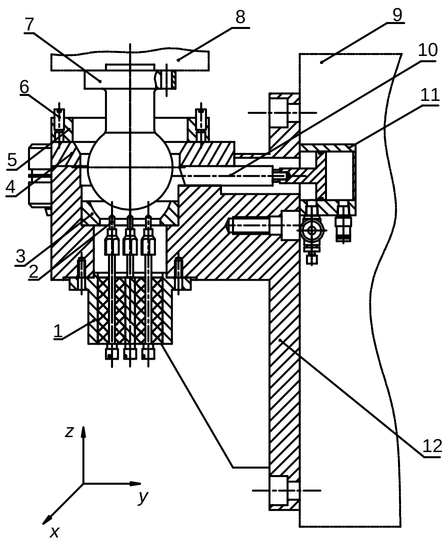

1: Sensor fixation apparatus; 2: Displacement sensor; 3: Ball-socket; 4: Pressure plate; 5: Laser emitter support; 6: Laser emitter; 7: Ball-head; 8: Transition joint; 9: Localizer; 10: Locking pin; 11: Fine lock cylinder; 12: Support plate

Fig. 1 Structure of the device

Firstly, we measure the ball-head's diameter and the distance between sensors with a micrometer or vernier caliper. Then we move a standard ball-head into the ball-socket of the localizer perpendicularly, and record the displacement sensor readings while the ball-head and the ball-socket contact completely. Then the measured values are used as initial conditions for implementing the control program. In addition, a handwheel is used to help users to realize the leading support. The user chooses a localizer and the related motion parameters by push buttons, and then the localizer is driven by a pulse signal. The localizer's motion state and displacement sensors' values can be displayed on an LCD. Fig. 2 shows the relation between the handwheel and the control system.

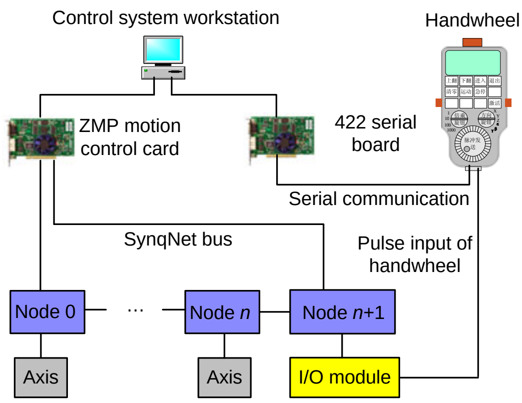

Fig. 2 Relation between the handwheel and the control system

Firstly, with the guidance of a laser array (i.e., laser column) structured by several emitters uniformly distributed on a column, the localizer is driven to reach the leading position by means of a handwheel, where the ball-head of the large aircraft component is enveloped in the laser column. The localizer is driven to move upward in the z direction until the ball-head touches at least one displacement sensor without interference, and then the control right of the motion is delivered from the handwheel to the control system. Secondly, the localizer is driven to move until the ball-head touches three or four displacement sensors by a recursive algorithm. The coordinates of the ball-head spherical center in a local coordinate system of the ball-socket are calculated by geometry. Furthermore, the spherical center deviations between the ball-head and the ball-socket are calculated. Finally, the localizer is driven to achieve a new position by compensation, and moves upward until the ball-head and the ball-socket contact completely when the deviation values satisfy the user-defined error limits. The remaining ball-heads of the large aircraft component gain their accurate support in the same way. In general, the large aircraft component's spatial position and pose are implemented by adjusting several localizers together. Fine lock cylinders are driven to clamp the ball-heads for subsequent work, such as joint, processing, and manually connection. The purpose of locking the ball-head is to apply a downward force on the ball-head, and the force can make the ball-head to contact with the ball-socket continuously in the assembly process. Three fine lock cylinders are symmetrically distributed along the centerline of the ball-socket. If the ball-head and the ball-socket contact completely (i.e., the spherical center of the ball-head is coincident with that of the ball-socket), the locking forces may counteract each other in the x and y directions. As a result, the residual force is not large enough to cause the ball-head to move in the horizontal plane.

Table 1 Key parameters of KTR auto-return series

KTR series	Measurement range (mm)	Linearity (%)	Repeatability (mm)	Driving force (N)
1	10	0.1		
2	25	0.1	0.01	≤3
3	50	0.09		

3 Key parameters design and reliability analysis

Key parameters, mainly including the arrangement of displacement sensors and the calculation of their mounting height, are considered. Necessary safety measures are also presented to improve the reliability of the device, such as prevention of zero drift and reservation of safety height.

3.1 Choice and calibration of displacement sensors

The displacement sensor should have the characteristics of high precision, self reset, anti-interference, and space saving.

MINOR KTR-10 sensor (signal output: 0–5V, 0–10V, ±5V, 4–20 mA) is a new kind of digital linear displacement sensor. Table 1 shows the key parameters of KTR auto-return series. The product is a potentiometer sensor, and it can send the continuous low-noise signals based on smooth movement. The displacement sensor, whose measuring head has a ball structure, can realize automatic reset by means of a built-in spring, and it is suitable for displacement measurement in restricted space.

Static calibration of the displacement sensor is shown in Fig. 3. A worktable is driven to move a standard value with a Kollmorgen servo motor. The corresponding displacement of the worktable is recorded using a Heidenhain grating ruler. The electrical signal of the displacement sensor is converted into a digital signal with slice I/O 6006 module.

Test data are produced with a reciprocating motion of the worktable. Calibration curves of four displacement sensors are obtained using the least square method, and the corresponding linear regression equations are obtained as follows:

$$y = 0.0023x + 1.2378, \tag{1}$$
$$y = 0.0026x + 0.8858, \tag{2}$$
$$y = 0.0025x + 0.7345, \tag{3}$$
$$y = 0.0024x + 0.7527, \tag{4}$$

where y is the input displacement signal and x is the output pulse signal in relation to the displacement sensor.

3.2 Arrangement of displacement sensors

When the ball-head sphere radius R is known, the coordinates of its spherical center can be calculated with only three points on its spherical surface in theory. Considering various errors, such as machining

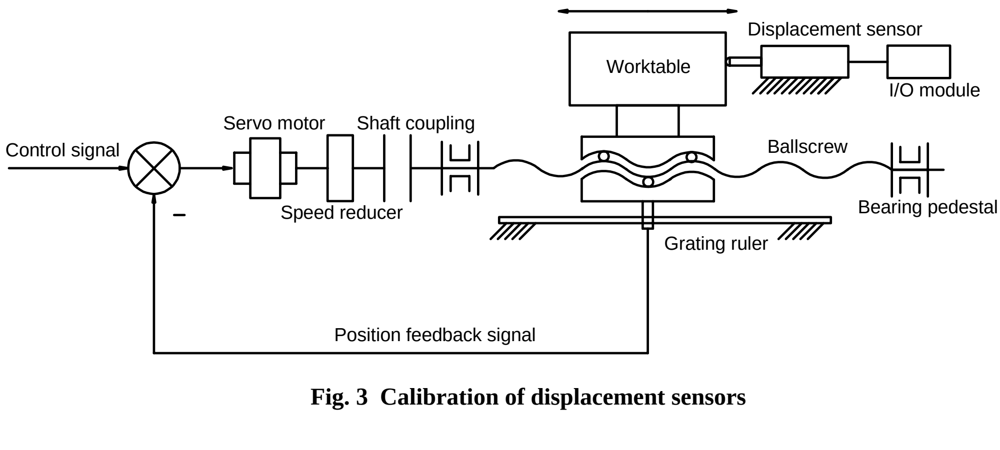

Fig. 3 Calibration of displacement sensors

and assembly errors of parts, and measurement and installation errors of the displacement sensors, the three points fitting to a sphere will create a large error. Conversely, the spherical equation solution with more points can effectively control the systematic error of the device, and shorten the calculation time of the ball-head spherical center. Considering all aspects of precision, efficiency, cost, and mounting space of the device, we choose four displacement sensors in all.

As shown in Fig. 4, a rectangular coordinate system *OXYZ* is established. Its origin is the ball-socket spherical center and its coordinate axes are three motion directions of the localizer. Four displacement sensors (marked as 1, 2, 3, and 4) are distributed uniformly on a circle whose radius is *r*, and *A*, *B*, *C*, and *D* are their measuring heads. The axes of displacement sensors are all on the planes *XOZ* or *YOZ*.

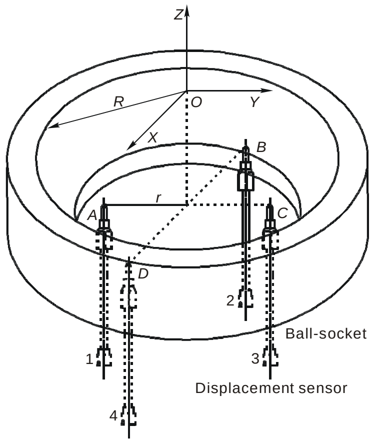

Fig. 4 Arrangement of displacement sensors

The value of *r* is determined by the factors below. The force of contact point between the ball-head and the measuring head of the displacement sensor is perpendicular to their spherical surfaces, and the reduction of *r* can control the lateral deformation of the measuring rod of the displacement sensor. The working region of the ball-head is subject to wear, so a small *r* can prevent the measuring head from touching the working area of the ball-head. Also, for a small *r*, there is the advantage of shortening the leading time of handwheel operation. Conversely, a large *r* is helpful in decreasing the fitting error. In applications, the value of *r* should be appropriate. When the radius of the ball-head *R* is 35 mm, *r* is recommended as 15 mm.

3.3 Mounting height calculation of displacement sensors

The ball-head must touch at least one displacement sensor before entering the ball-socket, so displacement sensors should be installed above their defined mounting height to guarantee the support safety.

As shown in Fig. 5, the axis deviation between the ball-head and the ball-socket should be less than 5 mm to prevent the ball-head from colliding with the support plate during the leading process. Point *E* is the critical interference point between the ball-head and the ball-socket. The distance between point *E* and the axis of the ball-socket *OZ* is 33.541 mm. Point *P* is the spherical center of the ball-head. Point *F* is the intersection of the ball-head axis *PF* and the ball-socket upper surface. Point *M* is the goal to which point *A* moves at the final stage of support. When the distance between the ball-head axis *PF* and the ball-socket axis *OZ* is equal to 5 mm, and plane *PEF* through the axis *OZ* bisects the fifth octant in the coordinate system *OXYZ*, the ball-head is most likely to collide with the ball-socket before touching any displacement sensor.

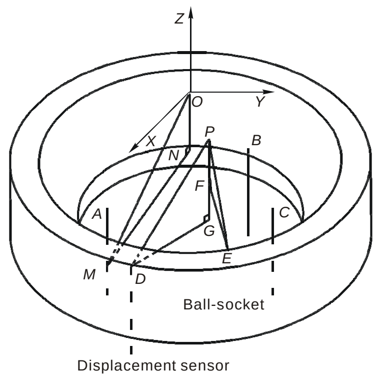

Fig. 5 Mounting height calculation model of displacement sensors

In the triangles *PEF* and *PDG*, some equations can be derived as

$$\begin{cases} PF = \sqrt{PE^2 - EF^2}, \\ PG = \sqrt{PD^2 - DG^2}, \\ FG = PG - PF, \end{cases} \tag{5}$$

where edges *PE* and *PD* are the radii of the ball-head, and $PE=PD=35$ mm. The distance between point E and edge PF, i.e., the length of EF, is 28.541 mm. The distance between point D and edge PF, i.e., the length of DG, is 11.997 mm. Then the length of FG is 12.621 mm. Thus the distance between the measuring head and the ball-socket upper surface should be less than 12.621 mm to guarantee the leading safety.

In the triangle OMN, edge ON can be derived as

$$ON=\sqrt{OM^2-MN^2}, \tag{6}$$

where the radius of the ball-head $OM=35$ mm. The distance between point M and OZ axis, i.e., the length of edge MN, is 15 mm. Then the length of ON is 31.623 mm.

The distance between point O and the ball-socket upper surface is 10 mm. The distance between point M and the ball-socket upper surface can be given as l=31.623−10=21.623 mm, and the least measurement range of the displacement sensor can be given as $d=l-FG$=21.623−12.621=9.002 mm. This indicates that the displacement sensor of KTR-10, whose measurement range is 10 mm, satisfies the requirement of the application.

3.4 Safety guarantee

The zero drift occasionally appears in the course of using sensors (Wu, 2008). Once the reading is falsely judged as its trigger signal, the localizer will be driven to move in a stochastic direction or even cause interference between the ball-head and the support plate. To avoid this hidden danger, firstly, we observe each reading before the large aircraft component is supported and adjust to zero. Secondly, a special checking program is assigned; i.e., if the reading exceeds a limiting value of zero drift, we consider that the ball-head has contacted with the measuring head of the displacement sensor.

In addition, it is found that the leading support error converges gradually to a small value. Before the large aircraft component gains its accurate support to form a ball joint, it often experiences two or more iterations; i.e., the coordinates of the ball-head spherical center are calculated, the localizer is adjusted to its specified position, and the support error is examined. This process is repeated until the ball-head enters into the ball-socket completely. Noticeably, a large spherical center deviation in the x or y direction may bring a lateral force to act on the large aircraft component. Therefore, height h is reserved when the localizer moves upward in the z direction and the localizer continues to move a distance of h until the positional deviations of three directions are all within each error limit.

4 Algorithm

4.1 Procedure description

In the process of leading the large aircraft component into the ball-socket by the ball-head, once at least one displacement sensor sends out a trigger signal, the subsequent work would be undertaken according to the recursive algorithm embedded in the control system without manual intervention. The steps of the algorithm are shown in Fig. 6. The displacement sensors should be installed in terms of the design layout and height to ensure that the ball-head touches at least one displacement sensor before hitting the ball-socket. To prevent the ball-head from laterally pressing the measuring rod of the displacement sensor, the localizer is driven to move along the track of “U”. The localizer descends until the displacement sensor’s measuring head detaches itself from the ball-head, approaches to the other untouched in the horizontal plane, and then moves upward. At the end of the leading process, the spherical center deviation between the ball-head and the ball-socket should satisfy the error limit at the height h as follows:

$$\begin{cases} |x_1-x_0|\le 0.05, \\ |y_1-y_0|\le 0.05, \\ |z_1-z_0-h|\le 0.05, \end{cases} \tag{7}$$

where x_1, y_1, and z_1 are the coordinates of the ball-head spherical center, and x_0, y_0, and z_0 are the coordinates of the ball-socket spherical center.

The maximum axis deviation between the ball-head and the ball-socket is 5 mm when the localizer reaches the leading position with the guidance of the laser column. In order to speed up the contact of three or more displacement sensors and the ball-head, the localizer moves in the horizontal plane with variable step size: the first step size, r/10=1.5 mm; the second step size, r/20=0.75 mm; and generally, 0.5 mm is taken as the step size when $n\ge 3$.

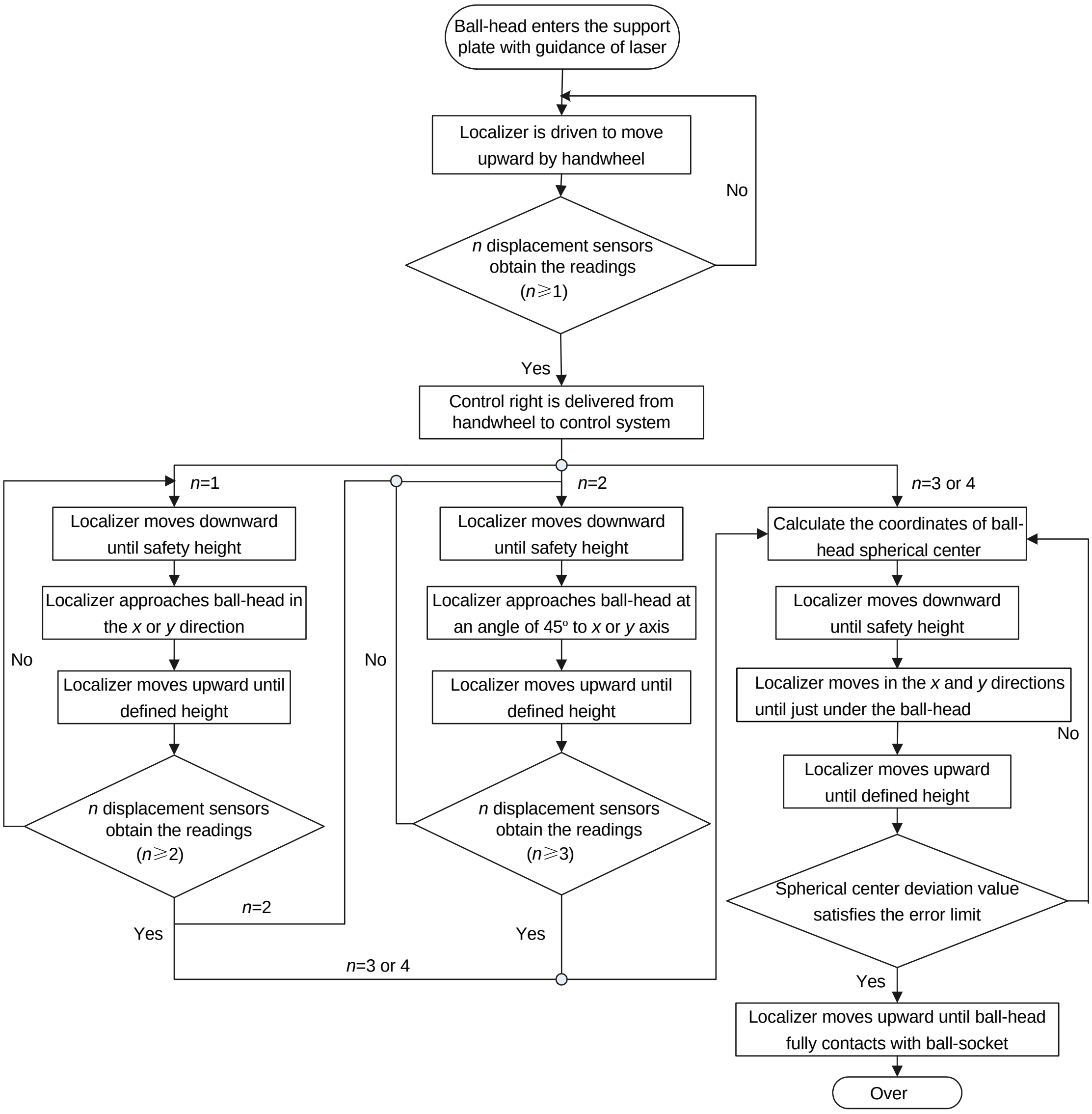

Fig. 6 Algorithm flowchart

4.2 Spherical center calculation of the ball-head

Sphere fitting accords with a nonlinear least square method from

$$\sqrt{(x-x_0)^2+(y-y_0)^2+(z-z_0)^2}-R=0. \quad (8)$$

Eqs. (9) and (10) can be derived from Eq. (8) by parameter transformation, and sphere fitting can be achieved using a linear least square method (Ke, 2005):

$$x^2+y^2+z^2+c_7x+c_8y+c_9z+c_{10}=0, \quad (9)$$

$$\begin{cases} x_0=-c_7/2, \\ y_0=-c_8/2, \\ z_0=-c_9/2, \\ R=\sqrt{c_7^2+c_8^2+c_9^2-4c_{10}}\Big/2, \end{cases} \quad (10)$$

where c_7, c_8, c_9, and c_{10} are spherical parameters. Here an algorithm model is proposed to calculate the ball-head spherical center based on three or four points and known radius, and a relatively simple geometric solution is chosen for it.

As shown in Fig. 7, points *A*, *B*, *C*, and *D* are the contact points between the measuring heads of displacement sensors and the ball-head. Firstly, the coordinates of A, B, C, and D are calculated according to initial installation positions and readings of the displacement sensors. Secondly, we arbitrarily choose three of these points, such as points A, B, and C, to form a triangle ABC. Then we arbitrarily select two edges of the triangle ABC, i.e., AB and BC, to construct planes perpendicular to each edge at the middle position. These vertical planes and plane ABC intersect at edges EF and EG, respectively. Edges EF and EG intersect at point E (i.e., circumcenter of the triangle ABC). Finally, point E moves a distance of EH ($EH=\sqrt{AH^2-AE^2}$) along the triangle ABC normal vector to obtain the coordinates of the ball-head spherical center H. We take the arithmetic mean of the coordinates of the ball-head spherical center, corresponding to the triangle ABC, ABD, ACD, and BCD, as the final result.

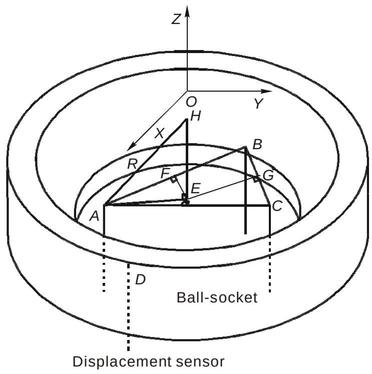

Fig. 7 Spherical center calculation of the ball-head

5 Results and discussion

The device for the large aircraft components gaining their accurate support by ball joint is shown in Fig. 8. The localizer moves at a speed of 1.5 mm/s in three different directions. In turn, the localizer is driven to touch displacement sensors in different combinations by means of a handwheel as follows: 1, 2, 3, 4, 1-2, 1-4, 2-3, 3-4, 2-3-4, 1-3-4, 1-2-4, 1-2-3, and 1-2-3-4. We take all these working conditions as initial conditions and record the positional relation between the ball-head and the ball-socket when contacted completely. Positional deviations between the ball-head and the ball-socket when contacted completely are given as

$$\begin{cases}\Delta x = x_1 - x_0,\\ \Delta y = y_1 - y_0,\\ \Delta z = z_1 - z_0 - h,\end{cases} \tag{11}$$

where Δx, Δy, and Δz are positional deviations of the spherical center between the ball-head and the ball-socket in the x, y, and z directions when supporting the test-fuselage, and here h is 4 mm. The results of the experiments are shown in Fig. 9.

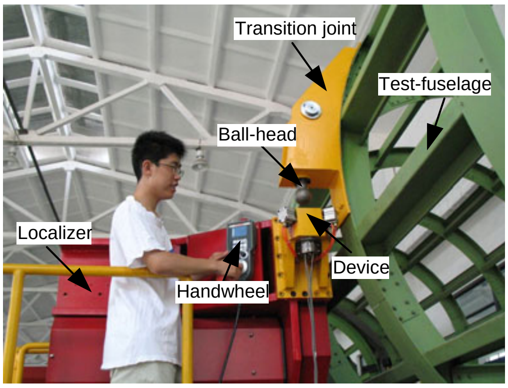

Fig. 8 Device for large aircraft components gaining accurate support by ball joint

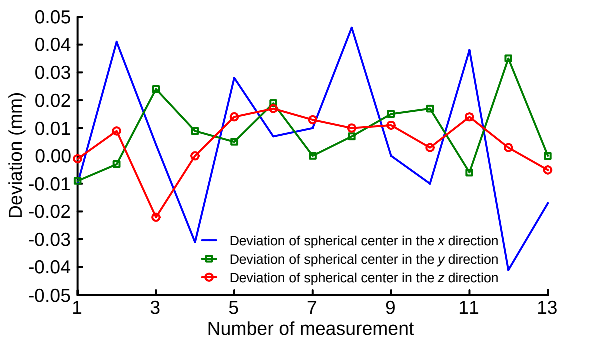

Fig. 9 Positional relation between the ball-head and the ball-socket while contacted completely

In the experiment, test-fuselage's spatial position and pose remain constant, and the space position of its ball-head is unique. No matter in which direction the localizer approaches the ball-head, the spherical center of the localizer's ball-socket will gradually converge to the same point according to the recursive algorithm. Record the space position of the ball-socket using the grating ruler of the localizer when supported. Positional deviations of the localizer's ball-socket are given as

$$\begin{cases} \mathrm{d}x = x_i - \dfrac{1}{13}\sum_{i=1}^{13} x_i \, (i=1, 2, \cdots, 13), \\ \mathrm{d}y = y_i - \dfrac{1}{13}\sum_{i=1}^{13} y_i \, (i=1, 2, \cdots, 13), \\ \mathrm{d}z = z_i - \dfrac{1}{13}\sum_{i=1}^{13} z_i \, (i=1, 2, \cdots, 13), \end{cases} \tag{12}$$

where dx, dy, and dz are positional deviations of the localizer's ball-socket in the x, y, and z directions when supporting the test-fuselage; x_i, y_i, and z_i are the coordinates of the ball-socket spherical center when supporting the test-fuselage. The results of the experiments are shown in Fig. 10.

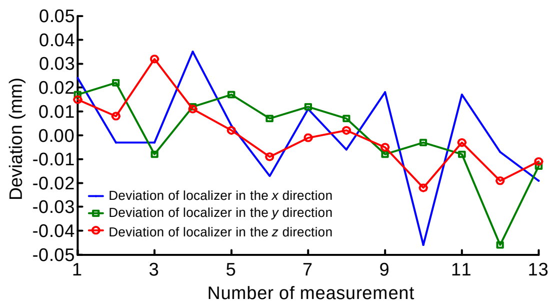

Fig. 10 Positional deviation of the localizer while contacted completely

The test-fuselage gains its accurate support and accords with various working conditions; i.e., the ranges of Δx, Δy, Δz, dx, dy, and dz in three different directions are all controlled within ±0.05 mm and their average errors (arithmetic mean of error absolute value) are controlled within 0.03 mm, as shown in Figs. 9 and 10. In the experimental data, the deviation in the x direction is the largest, the deviation in the y direction takes second place, and the deviation in the z direction is the third.

Support error of the test-fuselage is produced by a coupling system error of the device with positioning error of the localizer. The support precision of the test-fuselage has been controlled within the design positioning precision of the localizer (i.e., 0.05 mm/total travel in the x, y, and z directions). To conduct the test-fuselage's ball-head into the localizer's ball-socket with the help of the laser tracker, the support error is about 0.12 mm without considering the test-fuselage's deformation. The results of the experiments show that the system error of the device is small and the device can be widely used to lead the large aircraft components' assembly support. The spherical center of the localizer's ball-socket converging in a small area also shows the stability and reliability of the algorithm.

In the experiments, the time of leading the test-fuselage into its accurate support is also recorded, as shown in Fig. 11. The implementation time is controlled between 47 s and 122 s, and the average time is 79 s. The efficiency of the device is much higher than that of the laser tracker assistant method. We can conclude that it takes little time for the localizer to approach the ball-head until touching three or four displacement sensors, and the support time mainly depends on the times of spherical center calculation and localizer regulation. In the process of gaining an accurate support, motion displacement of the localizer in the z direction is much larger than those in the other two directions, and thus the efficiency of fulfilling the support mainly lies on the running speed of the localizer in the z direction.

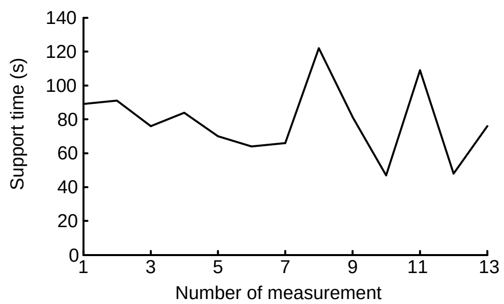

Fig. 11 Support time of the test-fuselage

6 Conclusions

To gain accurate support for large components in aircraft digital assembly, a new device is developed. Its key parameters are analyzed, and some safety measures are considered for the support reliability. A general recursive algorithm is proposed. The main issue is to simplify the program code and improve the program efficiency. Once some parameters of the algorithm are optimized further, it can be widely used in the leading support for the large aircraft components in assembly.

The results of the experiments show that the device has high precision and automation, provided that the proposed algorithm has good stability and convergence. It can ensure that the ball-head completely contacts with the ball-socket without bringing additional assembly stress in subsequent work, such as position and pose alignment, joint, and manually connection. The device has been successfully applied in two national key projects, and has a bright future in aircraft manufacture.

Acknowledgements

The first author would like to express his gratitude to Pu-jin HUANG, Wei-miao YAN, and Hui-qiang HU of Zhejiang University for their help in the experiments.

References

Fan, Y.Q., 2001. Manufacturing Technology of Modern Aircraft. Beijing University of Aeronautics and Astronautics Press, Beijing, China, p.56-57 (in Chinese).

Hartmann, J., Meeker, C., Weller, M., Izzard, N., Smith, A., Ferguson, A., Ellson, A., 2004. Determinate Assembly of Tooling Allows Concurrent Design of Airbus Wings and Major Assembly Fixtures. SAE 2004 Aerospace Manufacturing & Automated Fastening Conference & Exhibition, St Louis, MO, USA, 2004-01-2832.

Ke, Y.L., 2005. Theory, Method and System of CAD Modeling in Reverse Engineering. China Machine Press, Beijing, China, p.81-83 (in Chinese).

Kong, Z.Y., Huang, W.Z., Ceglarek, D., 2005. Visibility analysis for assembly fixture calibration using screen space transformation. *Journal of Manufacturing Science and Engineering*, **127**(3):622-634. [doi:10.1115/1.1947209]

Liu, J.H., Zou, C., 2008. A multi-aspect simulation system for flexible aircraft wing assembly. *Intelligent Robotics and Applications*, **5315**:679-687. [doi:10.1007/978-3-540-88518-4_73]

Naing, S., Burley, G., Odi, R., Corbett, J., 2001. Design for Jigless Assembly-Case Study of a Civil Airliner Fixed Leading Edge. 42nd AIAA/ASME/ASCE/AHS/ASC Structures, Structural Dynamics, and Materials Conference and Exhibit, Seattle, Washington, USA, p.1814-1824.

Naing, S., Corbett, J., 2004. Feature Based Design for Jigless Assembly. PhD Thesis, Cranfield University, Bedfordshire, UK.

Saadat, M., Cretin, L., 2002. Measurement systems for large aerospace components. *Sensor Review*, **22**(3):199-206. [doi:10.1108/02602280210433025]

Sun, W., Wei, Z.Z., Cao, L.J., 2009. A Triple-Laser Trackers Automatic Measurement System for Large-Scale Parts Assembly. 9th International Conference on Electronic Measurement & Instruments, Beijing, China, p.2-540-2-543. [doi:10.1109/ICEMI.2009.5274530]

Williams, G., Chalupa, E., Rahhal, S., 2000. Automated positioning and alignment systems. *SAE Transactions*, **109**(11):737-745.

Wu, J.P., 2008. Principle and Application of Sensor. China Machine Press, Beijing, China, p.13 (in Chinese).

Xiong, R.B., Ke, Y.L., Huang, P.J., 2009. An Adaptive Posture Following and Keeping Fixture Based on Aerostatic Bearing and Universal Ball Joint for Aircraft Digital Assembly. 13th International Manufacturing Conference, Dalian, China, p.623-628. [doi:10.4028/www.scientific.net/MSF.626-627.623]

Zhang, B., Yao, B.G., Ke, Y.L., 2009. A novel posture alignment system for aircraft wing assembly. *Journal of Zhejiang University-SCIENCE A*, **10**(11):1624-1630. [doi:10.1631/jzus.A0820777]